

Nd-Sr Isotopic Geochemistry and U-Pb Geochronology of the Fé Granitic Gneiss and Lajedo Granodiorite: Implications for Paleoproterozoic Evolution of the Mineiro Belt, Southern São Francisco Craton, Brazil

Wilson Teixeira¹ (wteixeir@usp.br), Ciro Alexandre Ávila² (avila@mn.ufrj.br),
Luciana Cabral Nunes³ (luciana@igc.usp.br)

¹Centro de Pesquisas Geocronológicas - Instituto de Geociências - USP
R. do Lago 562, CEP 05508-080, São Paulo, SP, BR

²Departamento de Geologia e Paleontologia - Museu Nacional - UFRJ, Rio de Janeiro, RJ, BR

³Programa de Pós-graduação - Instituto de Geociências - USP, São Paulo, SP, BR

Received 23 April 2007; accepted 12 March 2008

Keywords: Fé granitic gneiss, Lajedo granodiorite, U-Pb geochronology, isotopic geochemistry, Mineiro belt, tectonics.

ABSTRACT

The Fé granitic gneiss and Lajedo granodiorite belong to a voluminous felsic-mafic plutonism, tectonically linked to Paleoproterozoic magmatic evolution of the Mineiro Belt, southern portion of the São Francisco Craton, central-eastern Brazil. The Fé pluton is located north of the Lenheiros shear zone and is intrusive with respect to the Rio das Mortes greenstone belt and pyroxenite - gabbroic bodies, as indicated by xenoliths of gneiss and amphibolite, in the first case, and pyroxenite in the latter. The Lajedo granodiorite is located south of the Lenheiros shear zone and cuts the metamorphic rocks of the Forro peridotite – pyroxenite and mafic and intermediate rocks of the Nazareno greenstone belt, as evidenced by xenoliths from the latter unit. The modal composition of the Fé granitic gneiss lies within the ranges of monzogranite and syenogranite. It is peraluminous and shows a large variation in K₂O content, which implies a middle-K calc-alkaline to high-K calc-alkaline tendency. The Lajedo modal composition is consistent with granodioritic and tonalitic compositions. It indicates a predominantly peraluminous composition and calc-alkaline character. The U-Pb zircon crystallization age of the Fé granitic gneiss is 2191 ± 9 Ma, whereas the Lajedo granodiorite yields 2208 ± 26 Ma. The Nd/Sr characteristics of the Fé and Lajedo plutons are consistent with mixtures of enriched mantle (EMI-type), DMM and crustal components during magma genesis in a plutonic arc setting, while the low ⁸⁷Sr/⁸⁶Sr ratios point to contribution of mafic rock protoliths during magma genesis. This is also in accordance with the characteristic xenoliths observed within the investigated plutons from the Nazareno and Rio das Mortes greenstone belts. The Fé granitic gneiss and Lajedo granodiorite show tectonic characteristics which are comparable to those of nearby coeval plutons: Brito quartz-diorite (2221 ± 2 Ma), Brumado de Cima granodiorite (2219 ± 2 Ma), Brumado de Baixo granodiorite (2218 ± 3 Ma), Gloria quartz-monzdiorite (2188 ± 29 Ma), Cassiterita Trondjemite/Tonalite (2162 ± 10 Ma), Rio Grande diorite (2155 ± 3 Ma), Brumado diorite (2131 ± 4 Ma) and Ritápolis granite (2121 ± 7 Ma). As a whole, the integrated data and geologic setting of the plutons in the Mineiro belt define a well-constrained pre- to syntectonic phase of the Mineiro Belt to the period between 2221 and 2121 Ma.

Palavras-chave: Gnaisse granítico Fé, Granodiorito do Lajedo, geocronologia U-Pb, geoquímica isotópica, cinturão Mineiro, tectônica.

RESUMO

O gnaisse granítico Fé e o granodiorito do Lajedo são plutões felsicos associados à evolução paleoproterozóica do Cinturão Mineiro na porção sul do Cratão São Francisco. O plutão Fé está localizado ao norte da zona de cisalhamento do Lenheiro – importante feição estrutural associada a falhas compartimentando regionalmente o cinturão Mineiro. Esta intrusão possui xenólitos de gnaisse e anfíbolito do *greenstone belt* Rio das Mortes e de rochas máficas de corpos piroxénicos –

gabróicos que afloram nas proximidades. O granodiorito do Lajedo está localizado ao sul da zona de cisalhamento do Lenheiro, possui xenólitos de anfibolito do *greenstone belt* Nazareno e é intrusivo nas rochas metamáficas do corpo peridotítico - piroxenítico Forro e em rochas anfibolíticas do *greenstone belt* Nazareno. A composição modal do gnaisse granítico Fé é variável, de monzogranito a sienogranito; o plutônio é peraluminoso e apresenta conteúdos de K₂O compatíveis com tendências cálcio-alcalina médio K e cálcio-alcalina alto K, enquanto o plutônio do Lajedo varia de granodiorítico a tonalítico, é peraluminoso e tem natureza cálcio-alcalina. O gnaisse granítico Fé possui idade U/Pb em zircão de 2191 ± 9 Ma e o granodiorito do Lajedo 2208 ± 26 Ma. Os isótopos de Nd e Sr dos dois corpos revelam que componentes crustais participaram da gênese dos protólitos em ambiente de arco plutônico, com proporções variáveis de componente juvenil (tipos DMM e EMI) de idade possivelmente paleoproterozóica. Em particular, as baixas razões iniciais ⁸⁷Sr/⁸⁶Sr encontradas para os dois plutões do cinturão Mineiro são consistentes com a participação de materiais maficos na gênese dos corpos estudados em vez de crosta profunda. Tectonicamente, os resultados geocronológicos, isotópicos e os dados geológicos do gnaisse granítico Fé e do granodiorito do Lajedo são compatíveis com etapas pré- e sintectônica do Cinturão Mineiro, quando foram gerados os corpos: quartzo diorito do Brito (2221 ± 2 Ma), o granodiorito Brumado de Cima (2219 ± 2 Ma), o granodiorito Brumado de Baixo (2218 ± 3 Ma), o quartzo monzodiorito Glória (2188 ± 29 Ma), o tonalito/trondhjemita Cassiterita (2162 ± 10 Ma), o diorito Rio Grande (2155 ± 3 Ma), o diorito Brumado (2131 ± 4 Ma) e o granito Cassiterita (2131 ± 7 Ma).

INTRODUCTION

Geological mapping of the Paleoproterozoic felsic and mafic plutons in the southernmost portion of São Francisco Craton is a difficult task due to the polyphase metamorphic and deformational events overprinting the primary features of these intrusive bodies and host rocks. The cases of the Fé granitic gneiss and Lajedo granodiorite illustrates such complexity, and has led previous investigators to interpret them as a single pluton (Quéméneur and Baraud, 1982; Trouw, Ribeiro, Paciullo, 1986; Pires, Ribeiro, Barbosa, 1990).

Nevertheless, recent detailed geological mapping carried out in the São João del Rei region, in the Mineiro belt (e.g., Ávila, 2000; Ávila et al., 2006), with emphasis in the cartography of the felsic and mafic plutonic intrusions, has revealed that the Fé granitic gneiss and Lajedo granodiorite are individual bodies with distinctive composition. In addition they are truncated by the Lenheiros shear zone and crosscut different country rocks to the north and south of it. In this sense, this work deals with the petrographic and chemical characteristics of these plutons, which coupled with U-Pb zircon geochronology and Nd-Sr isotopic geochemistry provide new insights on the tectonic evolution of the Mineiro belt.

REGIONAL GEOLOGY

The geologic scenery of the southern border of the São Francisco craton comprises Archean and Proterozoic units integrating an Archean foreland and a Paleoproterozoic mobile belt (Figure 1), as summarized below (e.g., Teixeira et al., 2000; Noce et al., 2000):

a. Archean granulites, charnockites, enderbites, anortosites, gabbros and migmatized gneisses of Campo Belo, Bonfim, Belo Horizonte, Bação and Passa Tempo complexes (e.g., Carneiro, 1992; Noce, 1995; Teixeira et al., 1998; Cam-

pos, Carneiro, Basei, 2003), serpentinites, granodiorites, granites and Archean (Rio das Velhas Supergroup) and Nazareno greenstone belts – Machado and Carneiro, 1992; Noce, Machado, Teixeira, 1998; Machado et al., 1996; Noce et al., 2005; Hartmann et al., 2006);

b. Paleoproterozoic orthogneisses and migmatites and varied deformed and non-deformed intrusive plutons (Ávila, 2000; Cherman, 2004), as well as relicts of the Rio das Mortes greenstone belt. The latter unit is predominantly composed of amphibolites, gabbros and amphibolite-bearing schists interbedded with thick packages of queluzites, quartzites, phyllites and scarce metaultramafic rocks (Ávila, Teixeira, Pereira, 2004). Contrastingly the Nazareno greenstone belt which crops out as relicts in the study area exhibits abundant metaultramafic rocks (komatiites, serpentinites, talc-chlorite schists) and subordinated amphibolites and metasedimentary rocks, such as quartzites, gondites and phyllites (Ávila, 2000; Toledo, 2002; Ávila, Teixeira, Pereira, 2004);

c. Proterozoic supracrustals of different ages (Minas Supergroup and the Tiradentes, Lenheiro, Carandaí and Andrelândia sequences – Ribeiro et al., 1995).

The Paleoproterozoic domain – including the Mineiro belt – crops out along the southern São Francisco Craton, from the Quadrilátero Ferrifero towards the west, in the vicinities of Lavras (Alkmim, 2004). The belt evolution which was previously related with the Transamazonian orogeny (2.1-1.9 Ga) produced regional NE-SW trends and greenschist to amphibolite facies metamorphism overprinting the country rocks, as well as voluminous felsic and mafic plutonism. The crustal evolution of the Mineiro belt is compatible with accretionary orogens, as indicated by the variable $\epsilon_{\text{Nd(t)}}$ and $\epsilon_{\text{Sr(t)}}$ values (+1.3 to -11.0; +13 to +137 respectively; Noce et al., 2000) of the plutonic rocks and their calc-alkaline affinities (e.g., Ávila, 2000; Quéméneur and Noce, 2000; Teixeira et al., 2000). More recently, Teixeira

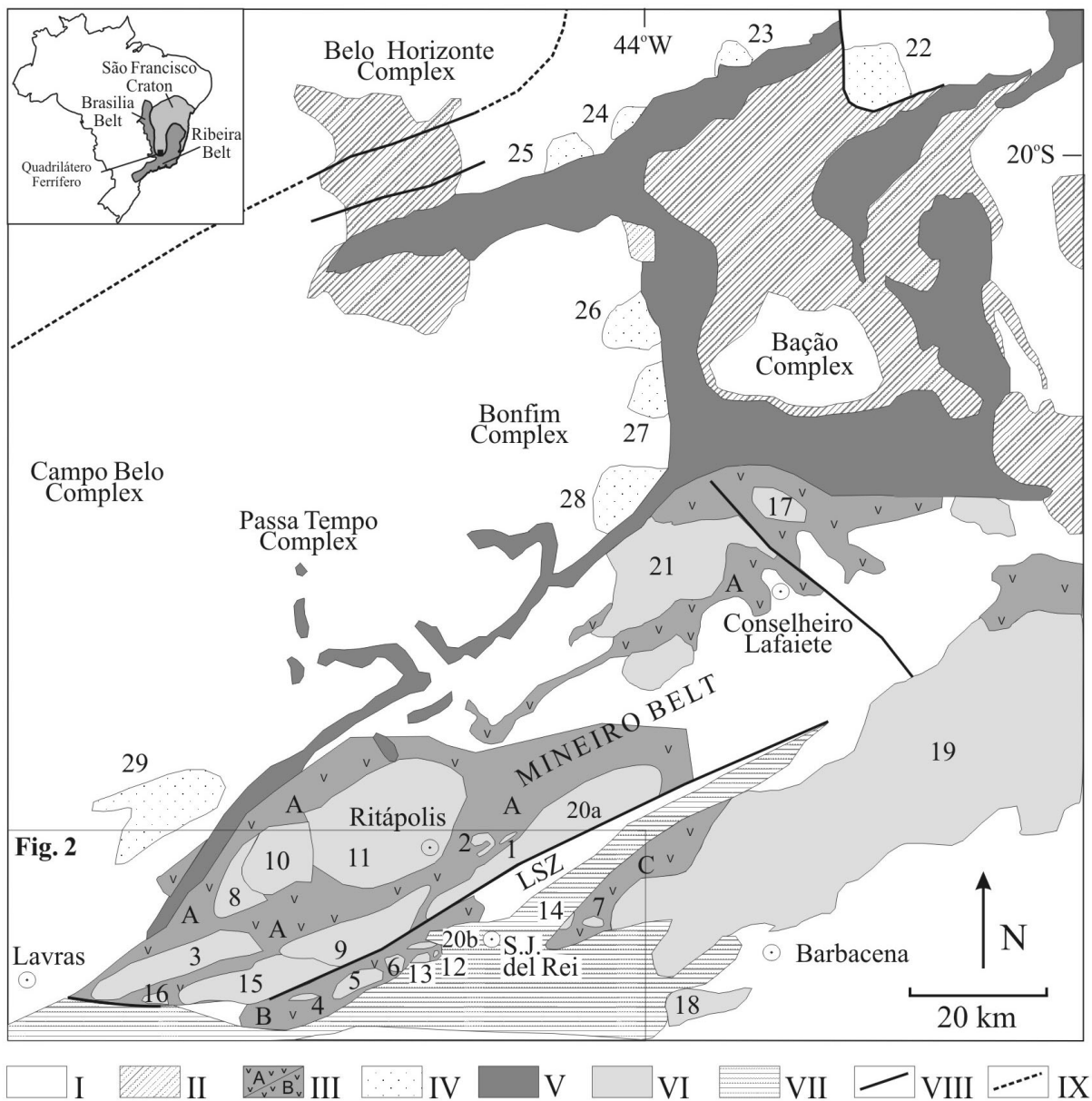


Figure 1. Geologic framework of the southernmost part of the São Francisco Craton (adapted from Ávila et al. 2003). **I.** Archean crust partly reworked during Paleoproterozoic times (Sul-Mineira province). **II.** Rio das Velhas greenstone belt (Archean). **III.** Archean/Paleoproterozoic greenstone belts: **A.** Rio das Mortes, **B.** Nazareno and **C.** Dores de Campos. **IV.** Archean granitoids. **V.** Minas Supergroup (Paleoproterozoic). **VI.** Paleoproterozoic felsic and mafic plutons. **VII.** São João del Rei (Paleoproterozoic), Carandaí (Mesoproterozoic) and Andrelândia (Neoproterozoic) supracrustal sequences. **VIII.** Major structures (e.g., Lenheiro shear zone; LSZ). **IX.** Limit of Sul Mineira Province. Paleoproterozoic plutons: **1.** Glória quartz-monzonodiorite, **2.** Brumado diorite, **3.** Rio Grande diorite, **4.** Rio Grande gabbro, **5.** São Sebastião da Vitória gabbro, **6.** Brito quartz-diorite, **7.** Vitoriano Veloso gabbro, **8.** Ibitutinga diorite, **9.** Cassiterita tonalite/trondhjemite, **10.** Tabuões trondhjemite, **11.** Ritápolis granitoid, **12.** Brumado de Baixo granodiorite, **13.** Brumado de Cima granodiorite and granophyric bodies, **14.** Tiradentes granitoid, **15.** Nazareno granite, **16.** Itumirim granitoid, **17.** Congonhas tonalite, **18.** Campolide granite, **19.** Ressaquinha complex, **20a.** Fé granitic gneiss, **20b.** Lajedo granodiorite, **21.** Alto Maranhão tonalite. Archean plutons: **22.** Caeté granodiorite, **23.** General Carneiro granite, **24.** Morro da Pedra granite, **25.** Ibirité granodiorite, **26.** Samambaia tonalite, **27.** Mamona granodiorite, **28.** Salto do Paraopeba granite.

et al. (2005) proposed the designation “Sul-Mineira Province” for such a large Paleoproterozoic domain in the southern part of the São Francisco Craton composed of gneisses, granitoids, supracrustal sequences, greenstone belts and mafic dikes, subjected to the Transamazonian metamorphism and deformation. According to this view the Mineiro belt makes up the southern part of the Paleoproterozoic domain, as mirrored by occurrence of the widespread coeval plutonic rocks.

The Paleoproterozoic framework of the Mineiro belt includes at least three distinct metamorphic-deformational events (as summarized in Table 1) in addition to a major regional structure – the Lenheiros shear zone (LSZ) and the Lenheiros and Rio das Mortes faults (Figures 1 and 2) – Avila, 2000; Avila et al., 2006). The LSZ separates distinct plutonic rocks either intrusive into the Rio das Mortes (in the north of shear zone) or into the Nazareno greenstone belts (in the south of LSZ) – such as the Fé granitic gneiss and Lajedo granodiorite to be dealt here. The latter unit comprises mainly metakomatiites and scarce, interlayered metapelites and quartzites, as well as amphibolites and andesites one of which yields $\epsilon_{\text{Nd(t)}}$ value of -1.0 and $^{87}\text{Sr}/^{86}\text{Sr}_{(t)} = 0.702$. Contrastingly in the Rio das Mortes greenstone belt metamafic rocks predominate associated with thick packages of queluzites, quartzites, phyllites. Two amphibolites of this unit yield $\epsilon_{\text{Nd(t)}}$ values of -1.5 and +0.1 ($^{87}\text{Sr}/^{86}\text{Sr}_{(t)}$ values of 0.700 and 0.701, respectively). As such the isotopic characteristics suggest the Rio das Mortes and Nazareno igneous rocks derived mainly from Paleoproterozoic magma sources (Teixeira et al., 2005).

Several plutons in the São João del Rei region have been previously investigated by means of geochronology, isotopic geochemistry and major, minor and trace element chemistry. They exhibit chemical compositions such as dominant metaluminous/peraluminous and calc-alkaline tendency whereas their emplacement ages are between 2255 and 2101 Ma (U-Pb and $^{207}\text{Pb}-^{206}\text{Pb}$ ages) – see location in Figures 1 and 2: Nazareno orthogneiss (2255 ± 6 Ma); Brito quartz-diorite (2221 ± 2 Ma); Brumado de Cima granodiorite (2219 ± 2 Ma); Brumado de Baixo granodiorite (2218 ± 3 Ma); Glória quartz-monzdiorite (2188 ± 29 Ma); Cassiterita tonalite/trondhjemite (2162 ± 10 Ma); Rio Grande diorite (2155 ± 3 Ma); Brumado diorite (2131 ± 4 Ma); Ritápolis granitoid (2121 ± 7 Ma); and Itumirim granitoid (2101 ± 8 Ma) – (Ávila, 2000; Ávila et al., 2003, 2005, 2006; Cherman, 2002, 2004). These plutons are linked with pre- and syn-tectonic stages of the Mineiro belt, as suggested from structural data and regional geologic inferences.

The plutons emplaced in the north of the LSZ show heterogeneous $\epsilon_{\text{Nd(t)}}$ values (from -1.0 to -3.3) suggesting that distinct components (in composition and age) have participated in the magma genesis, as also envisaged from

the varied T_{DM} ages (2.41-2.68 Ga) – Table 2. In contrast, the plutons located in the south of the shear zone have more homogeneous $\epsilon_{\text{Nd(t)}}$ values (most between -1.1 to -0.5) supporting they have a similar source, largely derived from juvenile (Paleoproterozoic) components (e.g., Teixeira and Ávila, 2007).

Fé granitic gneiss

The Fé pluton occurs between Ritápolis, Tiradentes and São João del Rei and crosscuts banded gneisses and the Rio das Mortes greenstone belt amphibolites. The intrusion exhibits an elongated exposure in accordance with the regional NEE/SWW trend foliation, whilst it is truncated along the southern edge by the Lenheiro fault (Figure 2). The outcrops display gneiss (Photo 1), amphibolite (Photo 2) and pyroxenite xenoliths that resemble, respectively, the typical lithologies of the nearby Rio das Mortes greenstone belt (Ávila, 2000) and the pyroxenitic-gabbroic bodies (Ávila et al., 1999). In addition, pegmatitic injections cut randomly the Fé granitic gneiss. It is noteworthy that orientation of muscovite and biotite from the pegmatite is parallel to the regional foliation (Photo 3), suggesting the Fé pluton is either pre- or syn-tectonic in relation to the main foliation.

The Fé rocks are whiteness to grayness in color, hololeucocratic, and fine to medium grained (0.2 to 1.5 mm). The mineral assemblage is: quartz, microcline, plagioclase, biotite, epidote, and accessory minerals like sphene, white mica, allanite, chlorite, zircon, carbonate, green hornblende, fluorite, apatite, opaque minerals (ilmenite, molibdenite, gold, pyrite and chalcopyrite), stilpnomelane and garnet (Table 3). Garnet and fluorite are magmatic phases, as suggested from the paragenesis with feldspar and biotite, whereas the presence of stilpnomelane is typical of low grade metamorphism (green schist facies). This rock shows usually white and grey bands (Photo 4) which may contain (rare) biotite and epidote. The modal composition is characteristic of monzogranitic and syenogranitic terms (Figure 3). The texture is dominantly inequigranular xenoblastic and subordinated porphyroblastic with plagioclase and microcline (perthitic) megacrystals up to 4 mm in size. The plagioclase has zircon inclusions, myrmekite intergrowth, is frequently altered to white mica, epidote and carbonate, as well as may be replaced by microcline. The biotite is hipidioblastic, brown and green and has zircon and allanite inclusions.

Lajedo granodiorite

The Lajedo granodiorite, likewise the Fé pluton, is strongly foliated in the NEE/SWW direction and contains amphibolite xenoliths. The latter rock is fine grained and porphyritic with plagioclase milemetric fenocrystals –

Table 1. Main characteristics of three recognized metamorphic-deformational events in the São João del Rei – Nazareno region.

Metamorphic event	Metamorphism	Mineralogy	Affected rocks
Paleoproterozoic I: 2250 – 2170 Ma (Ávila et al., 2006)	medium grade amphibolite facies	Mg-hornblende/Fe-hornblende + oligoclase or andesine ± chlorite ± epidote ± biotite ± sphene ± ilmenite (Cherman, 1999; Toledo, 2002)	Amphibolites, metakomatiites, schists, phyllites, gondites and quartzites (Nazareno and Rio das Mortes greenstone belts)
Paleoproterozoic II: 2131 – 2100 Ma (Ávila et al., 2006)	greenschist- and low-amphibolite facies	actinolite ± albite ± epidote ± biotite ± sphene (Ávila, 1992; Silva, 1996)	Amphibolites (Nazareno and Rio das Mortes greenstone belts); dunites, pyroxenites – gabbros; and Paleoproterozoic plutons
Neoproterozoic: 604 e 567 Ma (Söllner and Trouw, 1997; Trouw and Pankhurst, 1993)	greenschist to low amphibolite facies	Kyanite + biotite + chlorite + garnet + chloritoid + quartz + estaurolite (Ribeiro et al., 1995)	Quartzites, schists and phyllites of São João and Carandai megasequences. Development of NE-SW fault and shear zones

Table 2. SHRIMP U-Pb and $^{207}\text{Pb}/^{206}\text{Pb}$ ages, $\epsilon_{\text{Nd}(t)}$ and Sm-Nd T_{DM} model ages of selected plutonic rocks of the Mineiro belt. (1) SHRIMP U-Pb zircon age. (2) $^{207}\text{Pb}/^{206}\text{Pb}$ zircon evaporation age. $\epsilon_{\text{Nd}(t)}$ and $^{87}\text{Sr}/^{86}\text{Sr}_{(t)}$ values = crystallization age as indicated in the referred articles. LSZ = Lenheiros shear zone.

Plutons	Age (Ma)	$\epsilon_{\text{Nd}(t)}$	T_{DM} (Ga)	$^{87}\text{Sr}/^{86}\text{Sr}_{(t)}$	Relationship with LSZ	References
Glória quartz-monzonodiorite	2188 ± 29 ⁽¹⁾	-3.3	2.68	0.702	north	Ávila et al. (2006)
Cassiterita tonalite/trondhjemite	2162 ± 10 ⁽²⁾	-1.0	2.46	--	north	Ávila et al. (2003)
Rio Grande diorite	2155 ± 3 ⁽²⁾	-1.0	2.48	--	north	Cherman (2002)
Ritápolis granitoid	2121 ± 7 ⁽²⁾	-2.3	2.41	0.700	north	Ávila et al. (2006)
Brumado diorite	2131 ± 4 ⁽²⁾	-2.6	2.55	0.700	north	Ávila et al. (2006)
Nazareno orthogneiss	2255 ± 6 ⁽²⁾	-3.2	2.48	0.702	south	Cherman and Valença (2005)
Itutinga orthogneiss	2201 ± 5 ⁽²⁾	-1.1	2.31	0.702	south	Cherman (2002)
Brito quartz-diorite	2221 ± 2 ⁽²⁾	-0.6	2.63	0.700	south	Ávila et al. (2005)
Brumado de Cima granodiorite	2219 ± 2 ⁽²⁾	-0.5	2.51	0.700	south	Ávila et al. (2005)
Brumado de Baixo granodiorite	2218 ± 3 ⁽²⁾	-0.5	2.56	0.701	south	Ávila et al. (2005)

Photos 5 and 6). The Lajedo intrusion occurs in the south of the LSS, and crosscuts mafic and intermediate rocks of the Nazareno greenstone belt, as well the Forro peridotite – pyroxenite rocks (Figure 2) (Ávila, 2000).

The Lajedo rocks are grey in color, hololeucocratic, fine to medium grained, and granodioritic to tonalitic in composition (Figure 3). The main mineral assemblage is: quartz, plagioclase, biotite, microcline, epidote, and accessory minerals such as sphene, allanite, zircon, opaque minerals, white mica and chlorite (Table 3). Plagioclase is usually clouded by epidote and white mica, as a result from low grade metamorphism. The texture is dominantly inequigranular xenoblastic.

ANALITICAL PROCEDURES

Major, minor and trace elements of two samples from the Lajedo granodiorite and six samples from the Fé granitic

gneiss have been analyzed at the ICP-OES Laboratory, Institute of Geosciences, University of São Paulo (USP), Brazil. In addition, five samples of the Fé granitic gneiss have been analyzed at Lake-field Geosol Laboratory, Minas Gerais (Brazil). Samples were first powdered to < 200 mesh in an agate mill and results from both laboratories are similar within the error, as shown by analysis of a same sample (LC-04A and CT-141A) (Table 4).

The analytical routine of the USP laboratory comprises: X-ray fluorescence for the analyses of major and minor elements (SiO_2 , TiO_2 , Al_2O_3 , FeO_{tot} , MnO , MgO , CaO , K_2O , P_2O_5) using the melted pellets and X-ray fluorescence spectrometry (Philips PW2400) using pressed powder pellets for analyzing Ba , Rb , Sr , Zr , Y , Nb , Cu , Pb , Zn , Cr , F , Ga , Th and U trace elements. The routine of Lake-field laboratory comprises: X-ray spectrometry (Philips PW2400) for the analysis of the major and minor elements (SiO_2 , TiO_2 , Al_2O_3 ,

Table 3. Modal analyses [500 points (mean)] for samples of the Fé granitic gneiss and Lajedo granodiorite. (*) Protholiths. MG = Monzogranite. SG = Syenogranite. Tn = Tonalite. GD = Granodiorite. - = not observed. Tr = < 0.1%.

Sample	Fé												Lajedo										
	Pluton			CT			CT			CT			SS			SS			LJ				
	128	140	A	B	A	C	A	C	A	C	A	G	F	G	J	C	F	G	J	GD	CD	CD	
Classification (*)	MG	SG	MG	MG	SG	SG	MG	MG	SG	MG	MG	MG	MG	MG	MG	MG	MG	Tn	GD	GD	GD		
Plagioclase	21.9	20.9	23.4	20.6	16.6	21.6	22.2	22.2	16.8	28.3	21.9	28.0	25.8	30.8	30.9	54.6	54.8	52.9	53.4				
Quartz	30.5	35.4	37.0	37.8	36.6	24.8	31.1	29.9	34.6	39.4	36.4	38.8	35.6	38.2	25.0	23.2	35.6	33.5	31.2	30.2			
Biotite	4.5	1.6	1.3	0.7	1.5	5.0	1.9	3.5	Tr	5.4	0.3	0.5	1.2	1.3	2.9	3.4	4.2	3.5	4.8	3.5	3.3		
Microcline	37.7	39.0	36.1	36.6	41.7	44.1	38.0	38.1	43.3	23.3	30.9	35.5	31.6	30.7	37.8	36.4	1.1	5.2	7.5	8.1			
White mica	2.1	Tr	Tr	3.0	2.0	2.9	2.2	2.8	3.1	0.3	1.2	-	-	Tr	-	5.8	1.5	1.3	0.9	1.7			
Epidote	3.0	2.4	1.4	0.3	1.0	1.6	4.6	3.3	Tr	1.0	0.3	1.1	2.0	2.7	2.3	0.3	2.1	1.5	2.3	2.3	3.6		
Zircon	-	Tr	-	Tr	Tr	Tr	Tr	Tr	Tr	Tr	Tr	Tr	Tr	Tr	Tr								
Opaque minerals	Tr	0.6	0.4	1.0	0.6	-	Tr	Tr	1.5	0.7	1.9	1.1	Tr	Tr	0.3	-	Tr	Tr	Tr	Tr	Tr	Tr	
Allanite	-	Tr	0.4	Tr	Tr	Tr	Tr	Tr	Tr	0.7	0.3	1.1	Tr	Tr	0.3	-	Tr	Tr	Tr	Tr	Tr	Tr	
Apatite	-	-	-	-	-	-	-	-	-	-	-	Tr	Tr	-	-	-	-	-	-	-	-		
Sphene	0.3	0.1	Tr	Tr	Tr	Tr	Tr	Tr	0.2	0.7	0.3	Tr	Tr	Tr	0.6	-	0.9	0.2	0.4	0.6			
Hornblende	-	Tr	-	-	-	-	-	-	-	Tr	Tr	Tr	Tr	Tr	-	-	-	-	-	-	-		
Chlorite	-	Tr	-	-	-	-	Tr	Tr	-	Tr	Tr	Tr	Tr	Tr									
Garnet	-	Tr	Tr	-	Tr	-	-	-	-	Tr	Tr	Tr	0.4	Tr	Tr	-	-	-	-	-	-		
Stilpnomelane	-	-	-	-	-	-	-	-	-	Tr	0.3	Tr	1.2	1.3	-	-	-	-	-	-	-		
Fluorite	-	-	-	-	-	-	-	-	-	-	Tr	Tr	-	-	-	-	-	-	-	-	-		
Carbonate	-	Tr	Tr	-	-	Tr	Tr	Tr	-	2.1	Tr	-	Tr	Tr	-	-	-	-	-	-	-		

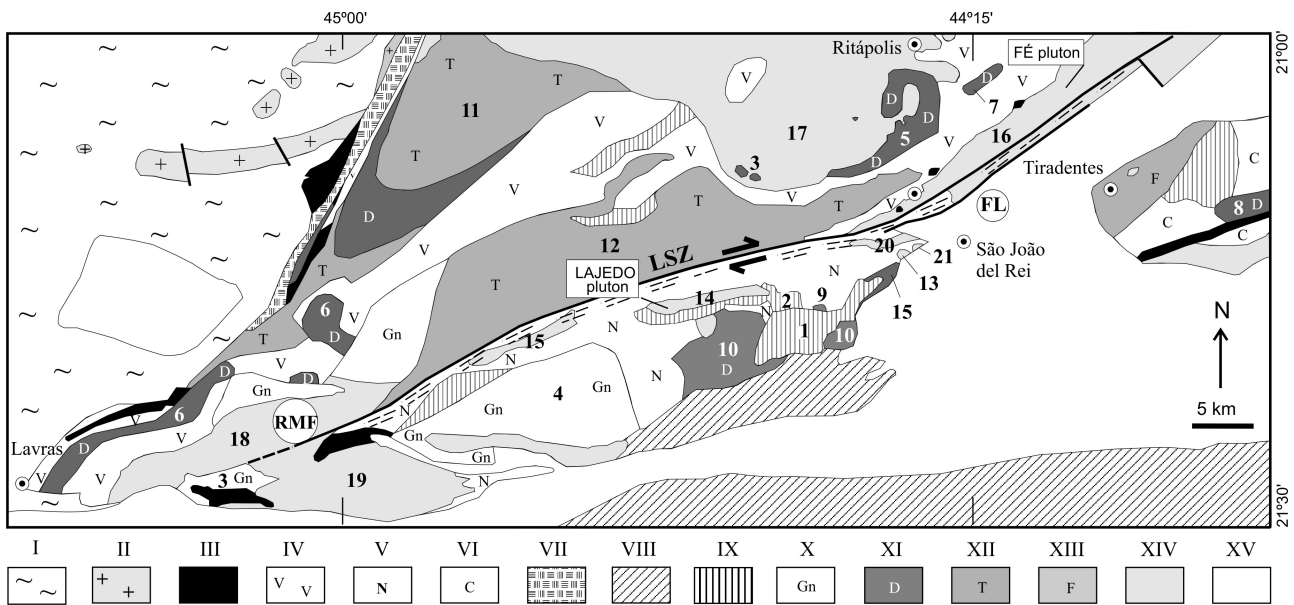


Figure 2. Geologic sketch between the cities of Lavras, São João del Rei and Tiradentes (adapted from Ávila et al., 2003; 2006). **Archean:** I. Undifferentiated gneiss, granulite, charnockite and mafic-ultramafic complexes; II. Granitoid rocks. **Archean/Paleoproterozoic:** III. Metaultramafic bodies; IV. Rio das Mortes greenstone belt; V. Nazareno greenstone belt; VI. Dores de Campos greenstone belt. **Paleoproterozoic:** VII. Minas Supergroup; VIII. Undifferentiated granitoid rocks; IX. Pyroxenite – gabbro: 1. São Sebastião da Vitória gabbro (2220 ± 3 Ma), 2. Forro Peridotite – Pyroxenite; X. Old orthogneiss: 3. Itumirim ortogneiss (2177 ± 4 Ma), 4. Nazareno orthogneiss (2255 ± 6 Ma); XI. Diorites, quartz-diorites e quartz-monzodiorites: 5. Brumado diorite (2131 ± 4 Ma), 6. Rio Grande diorite (2155 ± 3 Ma), 7. Glória quartz-monzodiorite (2189 ± 29 Ma), 8. Dores de Campos quartz-diorite (2199 ± 7 Ma), 9. Brito quartz-diorite (2221 ± 2 Ma), 10. Undifferentiated diorites and amphibolites; XII. Tonalites and trondhjemites: 11. Tabuões tonalite, 12. Cassiterita tonalite/trondhjemite (2162 ± 10 Ma); XIII. Metafelsites, metabasites and metasedimentary rocks; XIV. Granodiorites and granites: 13. Brumado de Cima granodiorite (2239 ± 25 Ma), 14. Lajedo granodiorite (2208 ± 26 Ma), 15. Nazareno granitoid, 16. Fé granitic gneiss (2191 ± 9 Ma), 17. Ritápolis granite (2121 ± 7 Ma), 18. Macuco de Minas granite (2116 ± 9 Ma), 19. Itumirim granite (2101 ± 8 Ma), 20. Brumado de Baixo granodiorite (2218 ± 4 Ma), 21. Granophyre and felsic volcanics (2207 ± 4 Ma). **Mesoproterozoic/Neoproterozoic:** XV. Supracrustal rocks of São João del Rei, Carandaí and Andrelândia mega-sequences. Faults: RMF (Rio das Mortes), FL (Lenheiro); Lenheiro shear zone (LSZ). See text for details.

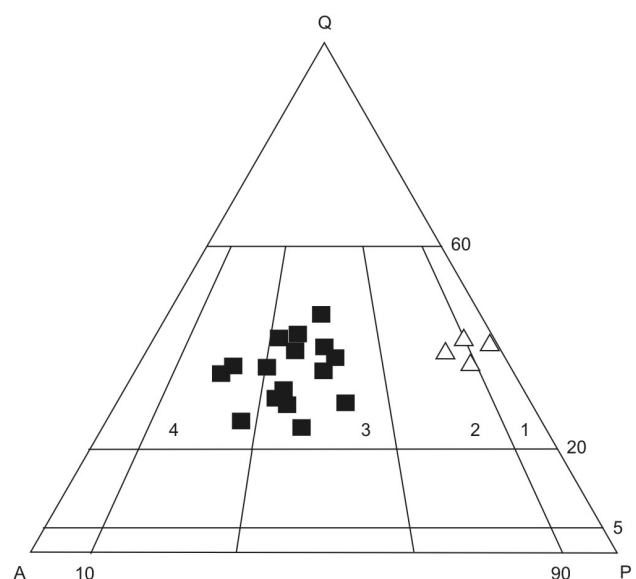


Figure 3. QAP diagram (Streckeisen, 1976) for the Fé granitic gneiss and Lajedo granodiorite. ■ = Fé granitic gneiss. △ = Lajedo granodiorite. 1. Tonalite. 2. Granodiorite. 3. Monzogranite. 4. Syenogranite.

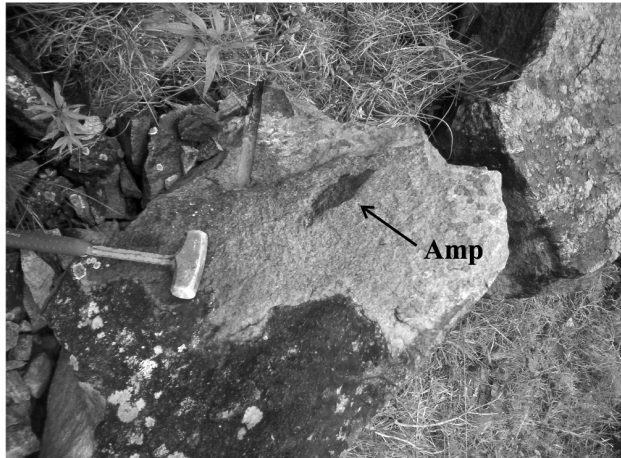


Photo 1. Elongated xenolith of amphibolite in the Fé granitic gneiss.

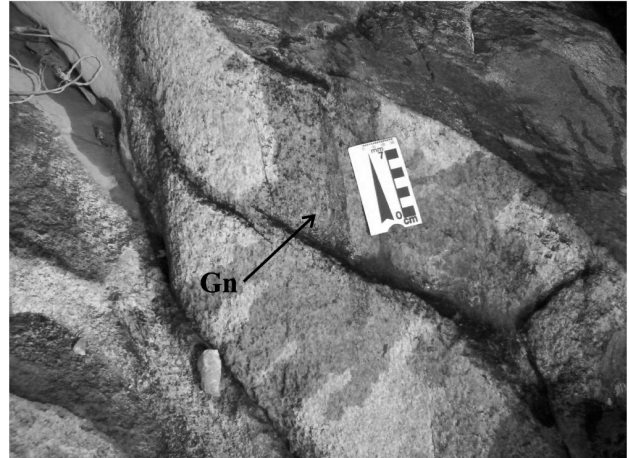


Photo 2. Elongated xenolith in the Fé granitic gneiss.



Photo 3. Orientation of biotite in pegmatite parallel to the trending foliation of the Fé granitic gneiss.

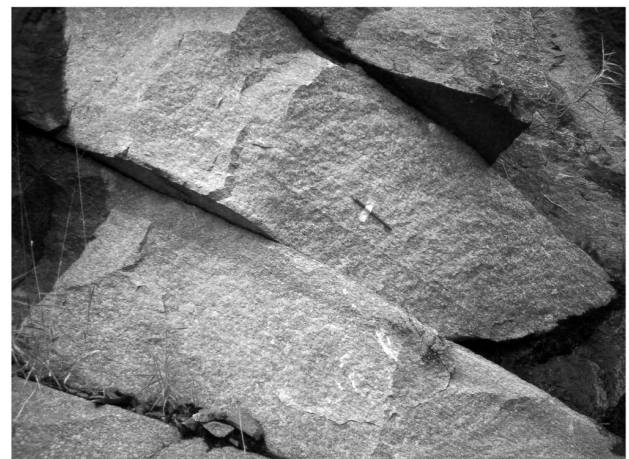


Photo 4. White and grey bands of the Fé granitic gneiss.

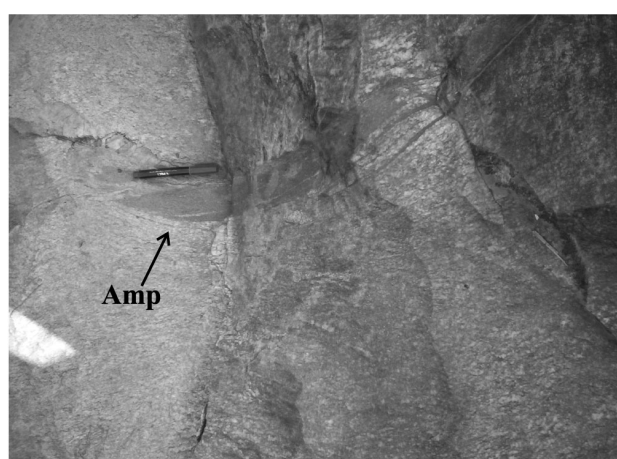


Photo 5. Elongated xenolith of amphibolite in the Lajedo granodiorite.



Photo 6. Xenolith of amphibolite with plagioclase fenocrystals in the Lajedo granodiorite.

FeO_{Tot}, MnO, MgO, CaO, K₂O, P₂O₅); atomic absorption spectrometry, after dissolution with HF + HClO₄ for Na₂O; decomposition with HF + H₂SO₄ in platinum crucible buffered for FeO with CO₂ evolution and FeO titillation with KMnO₄; loss of ignition by calcination at 1000°C under constant weight; X-ray fluorescence spectrometry using pressed powder pellets for Ba, Rb, Sr, Zr, Y, Nb, Cu, Pb and Zn. The samples to REE were analyzed by ICP-MS in the ICP Laboratory, Institute of Geosciences, University of São Paulo.

The U-Pb geochronology and Nd-Sr isotopic geochemistry were performed at the Geochronological Research Center (CPGeo) of the Institute of Geosciences – USP. The selected samples for U-Pb geochronology were crushed and further reduced to -100 and +250-mesh grain-sizes using a disc mill. The portion rich in heavy minerals was treated with bromoform and the heavy mineral concentrates were processed in a Frantz magnetic isodynamic separator at 0.5 Å. The non-magnetic fraction was treated with methyl

iodide ($d = 3.3 \text{ g/cm}^3$) and the fraction that contains the heavy minerals was once more processed in the Frantz separator at 1.0 and 1.5 Å, respectively. The final purification of the zircon fractions was carried out by hand picking under a stereomicroscope. The chemical dissolution of zircon was carried out with the addition of HF and HNO₃ within teflon microbombs (210°C; three days). Further details of the U-Pb analytical procedure are reported in Basei et al. (1995) with some additional improvements (e.g., usage of ²⁰⁵Pb spike). The isotopic composition of the samples, as well as the total Pb laboratory blank (7 pg during the period of the analyses) were determined in a Finnigan MAT 262 solid source mass spectrometer based on 2σ error statistics. After reduction of the data (PBDAT), the results were plotted in appropriate diagrams using the software ISOPLOT/EX (Ludwig, 2000).

Sm-Nd and Rb-Sr whole rock analyses were carried out using the two-column technique, as basically described by Sato et al. (1995). An ion exchange resin was used for primary separation of the REE, Rb and Sr, succeeded by a second HDEHP-coated teflon powder column, for separation of Sm and Nd elements. The isotope ratios were measured based on 2σ error statistics on the VG-354 multicollector mass spectrometer. The laboratory blanks for the chemical procedure during the period of analyses yielded maximum values of 0.4 ng for Nd and 0.7 ng for Sm. The average measurements of ¹⁴³Nd/¹⁴⁴Nd for the La Jolla international standard was 0.511857 (46) at the 2σ level. The Sm-Nd T_{DM} model ages were calculated using DePaolo (1981) and DePaolo, Linn e Schubert (1991) model parameters: $a = 0.25$, $b = -3.0$, $c = 8.5$ and ¹⁴⁶Nd/¹⁴⁴Nd = 0.7219 to normalize the isotope ratios [¹⁴³Nd/¹⁴⁴Nd = Nd(CHUR)₀ = 0.512638 and ¹⁴⁷Sm/¹⁴⁴Nd(CHUR)₀ = 0.1967]. The $\epsilon_{Nd(t)}$ values were calculated using the simplified equation $\epsilon_{Nd(t)} = \epsilon_{Nd(0)} - Q_{Nd} f_{Sm-Nd} T$, with the (CHUR)₀ values mentioned above and $Q_{Nd} = 25.09$.

RESULTS

Whole rock geochemistry

Tables 4 and 5 present major, minor and trace elements (including REE) analytical data from the studied plutons. The samples of Fé granitic gneiss show large variation in SiO₂ content (72.47% to 78.04% wt) and high K₂O contents (2.70% to 5.17% wt) when compared with Lajedo granodiorite: 71.79% to 72.66% wt (SiO₂) and 1.56% to 1.81% wt (K₂O) contents.

The Harker's diagrams for the Fé samples display negative correlations for Al₂O₃, CaO, Fe₂O_{3Tot}, MgO and positive for Na₂O (Figure 4). The low contents of CaO, MgO, Fe₂O_{3Tot}, Sr, Ni and Cr reflect the scarcity of calcic plagioclase and mafic phases (biotite and hornblende), as also revealed by the petrography. The Na₂O content of the Lajedo

Table 4. Chemical analyses of major (wt %), minor (wt %) and trace elements (ppm) for samples of the Fé granitic gneiss and Lajedo granodiorite. NA = not analyzed.

Samples	LC-01A	LC-01B	LC-02A	LC-03	LC-04A	LC-012C	CT-140A	CT-141A	CT-142A	CT-143C	CT-203	LC-06	LC-07
Pluton	Fé	Fé	Fé	Fé	Fé	Fé	Fé	Fé	Fé	Fé	Fé	Lajedo	Lajedo
Laboratory	USP	USP	USP	USP	USP	USP	Lakefield	Lakefield	Lakefield	Lakefield	USP	USP	USP
SiO ₂	74.16	72.47	74.93	75.71	78.21	73.51	75.30	76.70	77.30	74.90	77.30	71.79	72.66
TiO ₂	0.19	0.32	0.06	0.02	0.13	0.14	0.21	0.10	< 0.05	0.21	0.23	0.16	
Al ₂ O ₃	13.39	13.69	13.43	11.60	11.40	13.89	12.30	11.30	13.20	11.30	15.29	15.31	
Fe ₂ O ₃	0.04	0.17	0.43	0.51	1.17	0.10	1.10	0.93	0.87	0.43	1.30	0.46	0.32
FeO	1.37	2.08	0.69	1.76	0.60	1.26	1.90	1.60	1.90	1.30	1.10	1.14	1.10
MnO	0.03	0.04	0.03	0.06	0.04	0.03	0.05	< 0.05	< 0.05	< 0.05	0.02	0.02	
MgO	0.13	0.30	0.04	0.01	0.01	0.09	0.17	0.22	< 0.05	0.12	< 0.05	0.36	0.23
CaO	1.07	1.15	0.81	0.98	0.50	0.90	0.91	0.87	0.56	0.63	0.42	2.03	1.82
Na ₂ O	3.24	3.09	3.63	4.34	4.46	3.31	4.90	4.20	3.50	3.80	4.30	5.92	6.02
K ₂ O	5.10	5.06	4.83	3.11	3.00	5.17	2.90	2.90	2.70	4.70	3.40	1.56	1.81
P ₂ O ₅	0.05	0.06	0.03	0.01	0.01	0.05	0.04	0.04	< 0.05	0.07	0.11	0.07	0.04
PF	0.52	0.58	0.38	0.38	0.16	0.56	0.10	0.50	1.0	0.5	0.60	0.68	0.78
Total	99.29	99.01	99.29	98.49	99.69	99.01	99.88	99.43	99.23	99.65	100.04	99.55	100.27
Fe ₂ O ₃ tot.	1.48	2.48	1.20	2.47	1.84	1.50	2.89	2.44	2.68	1.69	2.27	1.73	1.54
Ba	765	786	202	1016	804	562	920	700	840	200	800	773	874
Rb	290	328	339	93	101	310	160	226	304	451	133	41	43
Sr	94	97	53	67	39	71	87	45	41	51	36	971	835
Zr	150	208	92	341	312	141	546	384	405	135	390	94	82
Y	31	37	40	71	73	38	107	154	75	64	102	4	5
Nb	12	20	21	20	17	17	< 9	< 9	< 9	< 9	< 9	< 9	< 9
Cu	4	4	4	23	4	3	5	30	35	5	5	5	< 5
Pb	39	48	58	16	16	61	< 20	20	20	80	30	10	12
Zn	33	60	38	90	128	43	85	35	60	40	35	50	48
Cr	< 5	16	< 5	28	7	20	NA	NA	NA	NA	NA	27	< 13
F	< 355	658	< 355	1082	< 355	NA	NA	NA	NA	NA	NA	< 550	< 550
Ga	18	22	22	19	20	20	NA	NA	NA	NA	NA	22	22
Th	42	68	38	7	6	48	NA	NA	NA	NA	NA	< 7	< 7
U	14	22	21	3	3	< 3	NA	NA	NA	NA	NA	15	14

Table 5. Chemical analyses of REE (ppm) for samples of the Fé granitic gneiss and Lajedo granodiorite. # = Fé granitic gneiss. Φ = Lajedo granodiorite.

Elements	LC-01B	LC-02A	LC-03	LC-013A	LC-06	LC-07
	#	#	#	#	Φ	Φ
La	96.97	24.72	58.00	70.67	11.2	8.29
Ce	184.95	59.87	119.87	144.01	21.5	13.8
Pr	18.34	5.96	13.74	13.56	2.61	1.92
Nd	60.53	20.47	51.54	44.14	8.9	6.63
Sm	10.61	5.20	10.20	8.00	1.71	1.66
Eu	0.77	0.30	1.62	0.44	0.52	0.44
Gd	8.36	5.01	9.27	6.39	0.88	0.93
Tb	1.16	0.91	1.56	1.03	0.10	0.13
Dy	5.93	5.74	9.97	5.84	0.50	0.66
Ho	1.17	1.21	2.34	1.23	0.11	0.14
Er	3.79	3.41	7.23	3.60	0.21	0.24
Tm	0.45	0.52	1.22	0.51	0.05	0.06
Yb	2.59	3.04	7.80	2.94	0.22	0.25
Lu	0.40	0.44	1.23	0.44	0.03	0.03

granodiorite samples (5.92 to 6.02% wt) is higher than in the Fé ones (3.09 to 4.46% wt). This variation is directly associated to the abundance of albite in the Lajedo granodiorite and the presence of microcline and albite in the Fé granitic gneiss. The latter samples have two different patterns of K₂O content (Figure 4).

The main chemical characteristics of the Fé granitic gneiss and Lajedo granodiorite indicate a sub-alkaline trend (Figure 5a), calc-alkaline tendency (Figure 5b) and predominantly a peraluminous and subordinately metaluminous composition (for the former) and peraluminous for the latter pluton (Figure 5c). The Fé samples show subordinate metaluminous tendency, as explained by the scarcity of hornblende. They fall in the calc-alkaline series field and in the high-K calc-alkaline to shoshonitic series fields (Figure 5d), in accordance with the large variation on K₂O contents, while the Lajedo samples plot in the calc-alkaline series field (Figure 5d). In the diagram Ab-An-Or (Figure 5e) the Lajedo samples plot in the trondhjemite field, while the Fé samples plot mainly in the granite field as well as in the limit of the granite and trondhjemite fields. It is also noteworthy that the contents of SiO₂, Al₂O₃, Sr, Y and Yb of the studied samples are compatible to high-Al₂O₃ trondhjemites or continental trondhjemites (e.g., Martin, 1987).

The high Rb (93 to 451 ppm) and Ba (200 to 1016 ppm) contents in the Fé granitic gneiss are associated with the presence of microcline (perthitic) whereas the low content of Sr (36 to 97 ppm) is related with the scarcity of calcic plagioclase. Contrastingly, the Lajedo granodiorite has low

Rb content (41 to 43 ppm) which is related with the scarce microcline and higher content in Sr (835 to 971 ppm) which is associated with the plagioclase phase.

The Fé and Lajedo plutons have low contents of HFS elements, such as Zr and Nb. These characteristics are comparable to those of high-K calc-alkaline suites from orogenic environments (Brown, Thorpe, Webb, 1984; Pearce, Harris, Tindle, 1984).

Chondrite normalized rare-earth elements patterns from samples showing inequigranular xenoblastic and porphyroblastic textures of Fé granitic gneiss present similar features (Figure 6), given by strong negative Eu anomalies, flat heavy rare earth distribution and high La/Y ratios. These features are associated with fractionation of feldspar, zircon and allanite. In contrast, the distribution of rare earth elements of Lajedo granodiorite shows depleted heavy rare earth pattern and low content of total rare earth. These features indicate fractionation of the hornblende, calcic plagioclase and zircon. Figure 7 shows patterns of incompatible element concentrations normalized to those of primitive mantle (Taylor and McLennan, 1985) for the Fé and Lajedo samples. The Sr, HFSE (Zr, P, Nb and Ti) and LILE (Ba and K) signatures are consistent with the geochemical features of volcanic arc-derived rocks, as indicated by Ti negative anomalies, and moderate Y and Nb contents. In addition, the investigated samples show Zr positive anomalies and strong P₂O₅ negative ones, indicating the presence of zircon and scarcity (Fé samples) or absence (Lajedo samples) of apatite, as revealed by the petrography.

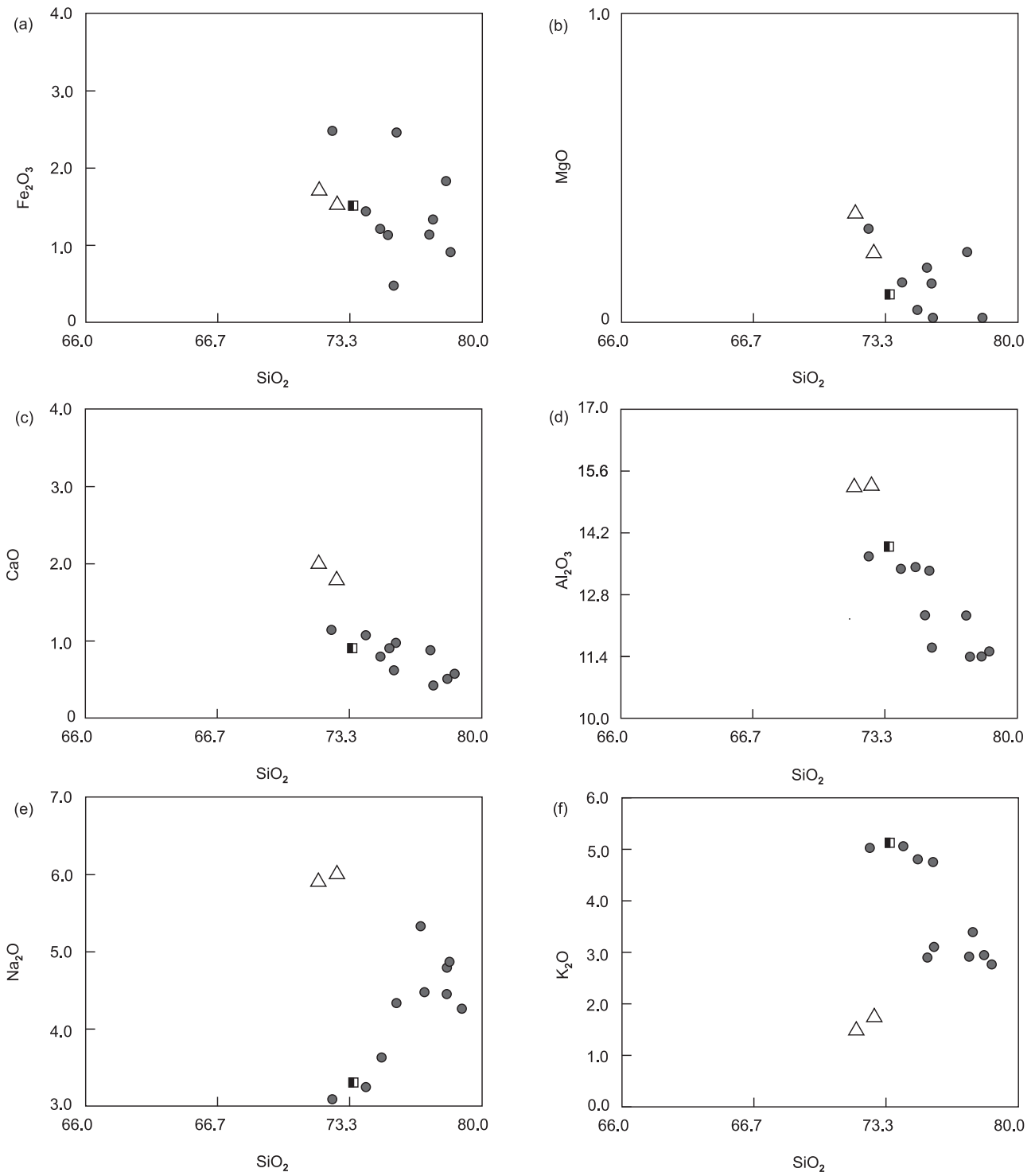


Figure 4. Major variation diagrams using SiO_2 as a differentiation index for the Fé granitic gneiss and Lajedo granodiorite. \triangle = samples with inequigranular xenoblastic texture (Lajedo granodiorite). ● = samples with inequigranular xenoblastic texture (Fé granitic gneiss). □ = samples with K-feldspar porphyritiblastic texture (Fé granitic gneiss).

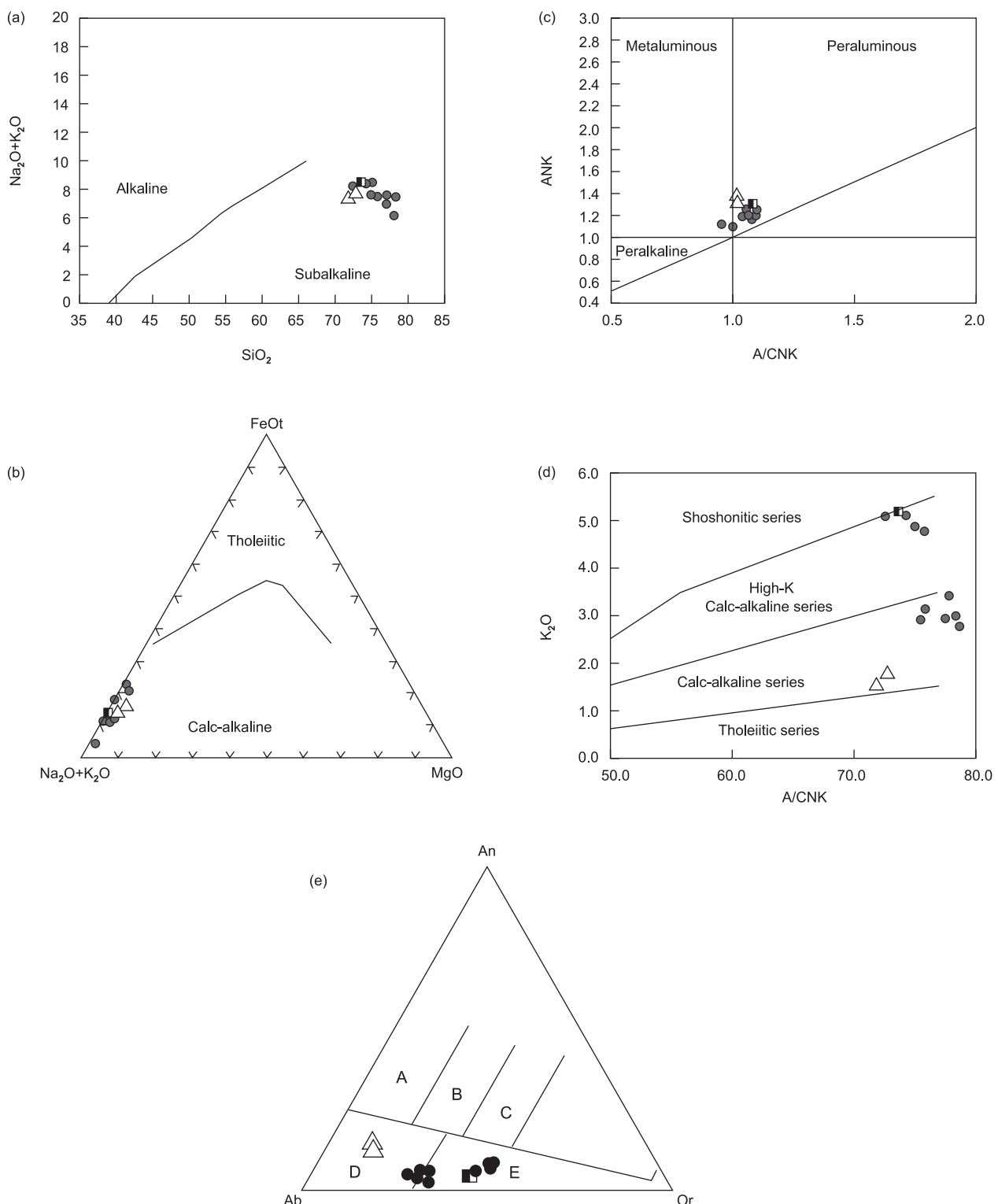


Figure 5. Discriminate diagrams for the Fé granitic gneiss and Lajedo granodiorite. **a** = $\text{SiO}_2 \times \text{Na}_2\text{O} + \text{K}_2\text{O}$ (Irvine and Baragar, 1971). **b** = $\text{MgO}-\text{FeO}^*-\text{Na}_2\text{O} + \text{K}_2\text{O}$ (Irvine and Baragar, 1971). **c** = $[\text{Al}_2\text{O}_3 / (\text{CaO} + \text{Na}_2\text{O} + \text{K}_2\text{O})]_{\text{mol}} \times [\text{Al}_2\text{O}_3 / (\text{Na}_2\text{O} + \text{K}_2\text{O})]_{\text{mol}}$ (Maniar and Piccoli, 1989). **d** = $\text{SiO}_2 \times \text{K}_2\text{O}$ (Peccirillo and Taylor, 1976). **e** = Ab-An-Or (O'Connor, 1965): **A**. tonalite, **B**. granodiorite, **C**. adamellite, **D**. trondhjemite, **E**. granite. Symbols as in Figure 4.

U-Pb geochronology

The Fé granitic gneiss contains two zircon populations, both showing frequent inclusions:

1. one of them varies from elongated, prismatic crystals with well-developed pyramidal termination and colorless (Figure 8a) to short and small prismatic zircons (Figure 8b), well-developed pyramidal termination and colorless;

2. the other zircon population exhibits short crystals with well-developed pyramidal termination, dark color, and dirty aspect (Figure 8c). However, this population was not selected for U-Pb dating because of a probable high U content and

high degree of metamictization, as suggested by the dark aspect of the zircons.

Table 6 presents the analytical data of the zircon population (1) dated by U-Pb TIMAS geochronology. Among the eight analyses performed (LC-01B A; LC-01B B; LC-01B C; LC-01B D; LC-01B E; LC-01B F; LC-01B G; LC-01B H) two of them were excluded for the age calculation due to the very low radiogenic Pb (i.e., anomalous $^{206}\text{Pb}/^{204}\text{Pb}$ ratios; lab. numbers: 3103; 3106). The six selected analyses define a discordia/concordia intercept (Figure 9) at 2191 ± 9 Ma which is interpreted as the crystallization age of the Fé granitic gneiss.

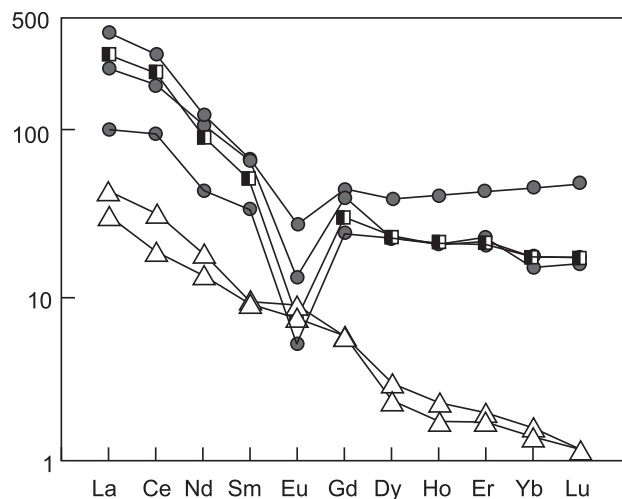


Figure 6. Distribution of the rare earth elements normalized to chondrite pattern of Boynton (1984). Symbols as in Figure 4.

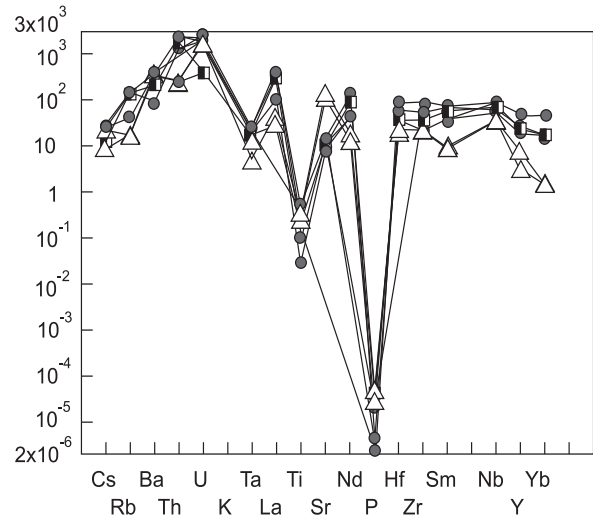


Figure 7. Spidergram of selected samples, normalized to primitive mantle (Taylor and McLennan, 1985). Symbols as in Figure 4.

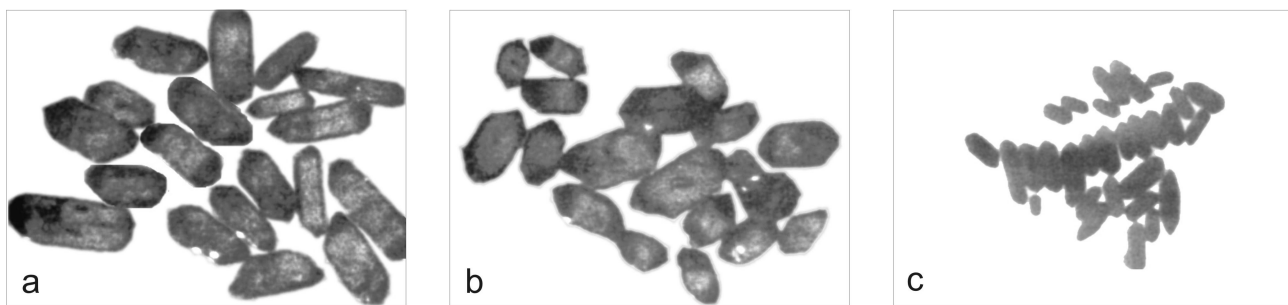


Figure 8. Zircon types from the Fé granitic gneiss. **a.** Colorless, elongated and prismatic zircons with well-developed pyramidal termination. **b.** Colorless, short and prismatic zircons with well-developed termination. **c.** Dark, short and prismatic crystals zircon with rounded terminations. Zircon types (a) and (b) have been selected for U-Pb TIMS dating.

Table 6. U-Pb data of LC 01 sample (Fé granitic gneiss). See text for details. Zircon (Zr) types: **1.** elongated, prismatic crystals with well-developed pyramidal termination and colorless; **2.** to short and small prismatic zircons with well-developed pyramidal termination and colorless. * = not corrected for blank or non-radiogenic Pb. # = radiogenic Pb corrected for blank and initial Pb. **U** = radiogenic Pb corrected for blank. **#** = corrected for blank.

Lab number/ Zircon fraction	Zr type	Weight (mg)	U (ppm)	Pb (ppm)	$^{206}\text{Pb}/^{238}\text{U}$	#	$^{206}\text{Pb}/^{238}\text{U}$	Error (%)	#	$^{207}\text{Pb}/^{235}\text{U}$	Error (%)	#	$^{207}\text{Pb}/^{235}\text{U}$	Error (%)	Age (Ma)	Age (Ma)	Age (Ma)	Age (Ma)	Coef.
3101/LC 01B M(-1)A	1	0.036	361.6	136.1	10323.6	0.346211	0.743	6.38745	0.477	0.133809	0.0612	1917	2031	2149	0.991745				
3104/LC 01B M(-1)D	1	0.036	293.0	115.8	912.5	0.345778	0.485	6.35687	0.491	0.133335	0.0788	1914	2026	2142	0.987053				
3105/LC 01B M(-1)E	2	0.022	355.7	133.4	8865.4	0.345678	0.470	6.34851	0.473	0.133198	0.0555	1914	2025	2141	0.993080				
3107/LC 01B M(-1)G	2	0.023	445.1	166.3	11850.3	0.342872	0.684	6.32622	0.712	0.133817	0.1950	1901	2022	2149	0.961708				
3108/LC 01B M(-1)H	1	0.028	394.4	146.9	4351.8	0.341559	0.781	6.27906	0.818	0.133330	0.2380	1894	2016	2142	0.955616				
3102/LC 01B M(-1)B	1	0.331	308.4	64.0	5726.6	0.195357	0.472	3.09631	0.477	0.114951	0.0631	1150	1432	1879	0.991212				
3103LC_01B M(-1)C	1	0.045	216.6	69.6	112.1	0.195409	5.170	3.01982	6.980	0.112082	4.21	1151	1413	1833	0.80022				
3106/LC 01B M(-1)F	2	0.032	227.0	107.5	261.5	0.354607	1.110	6.46318	1.910	0.132189	1.42	1957	2041	2127	0.67622				

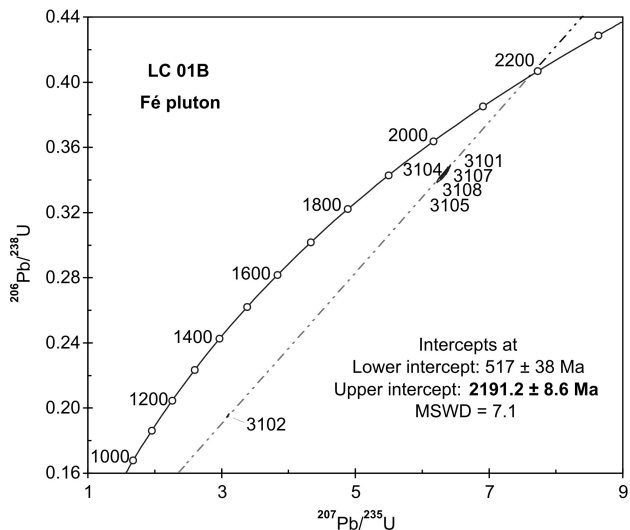


Figure 9. U-Pb diagram of LC-01B sample (Fé granitic gneiss). See text for details.

The Lajedo granodiorite contains three zircon populations:

1. small prismatic zircons with rounded terminations (colorless), with frequent inclusions (Figure 10a);
2. small prismatic zircons with rounded terminations (white color). They contain frequent inclusions, and are dirty in aspect which is probably due to metamictization (Figure 10b);
3. prismatic colorless zircons with rounded terminations and showing few inclusions (Figure 10c).

Among the five zircon fractions from these populations selected, four of them (A, B, C, D) were dated by U-Pb TIMS geochronology (Table 7; Figure 11). The discordia/concordia intercept of 2208 ± 26 Ma is interpreted as the minimum crystallization age of the Lajedo granodiorite, due to the observed discordance. However, analysis A (zircon population 3) which plots closest with the concordia, yields a $^{207}\text{Pb}/^{206}\text{Pb}$ model age of 2205 ± 1.3 Ma. This is also an estimated age of the Lajedo pluton due to the magmatic aspect of the analyzed prismatic zircons. Meanwhile the large error of the linear array is basically due to variable Pb radiogenic losses of each particular zircon fraction.

Nd-Sr isotope geochemistry

Sm-Nd and Rb-Sr whole rock analyses of the Fé granitic gneiss and Lajedo granodiorite and their initial Nd and Sr isotopic parameters (Tables 8 and 9) were plotted in an isotopic correlation diagram (Figure 12) which also includes

Table 7. U-Pb data of LC-06 sample (Lajedo granodiorite). See text for details. Zircon (Zr) types: **1.** Small prismatic zircons with rounded terminations (colorless), with frequent inclusions. **2.** Small prismatic zircons with rounded terminations (white color), dirty in aspect, with frequent inclusions. **3.** prismatic colorless zircons with rounded terminations, with few inclusions (Figure 10c). **#** = radiogenic Pb corrected for blank and initial Pb. **U** = corrected for blank or non-radiogenic Pb.

Lab number/ Zircon fraction	Zr type	Weight (mg)	U (ppm)	Pb (ppm)	#		#		#		#		
					$^{206}\text{Pb}/$ ^{238}U	Error (%)	$^{207}\text{Pb}/$ ^{235}U	Error (%)	$^{207}\text{Pb}/$ ^{238}U	Error (%)	$^{206}\text{Pb}/$ ^{235}U	Error (%)	
3245/A	3	0.01157	222.8	102.02	1834.74	0.392734	0.54	7.485570	0.54	0.138237	0.07	2136	2171
3246/B	1	0.0299	204.1	50.80	2646.27	0.245516	0.50	4.370890	0.50	0.129119	0.06	1414	1707
3247/C	1	0.00147	124.5	38.53	1562.03	0.298011	0.58	5.449810	0.58	0.132631	0.10	1681	1893
3248/D	2	0.0231	145.2	49.77	2117.25	0.333433	0.53	6.197080	0.53	0.134796	0.06	1855	2004
3249/E	2	0.01049	65.6	22.60	1029.83	0.317942	0.85	5.792800	0.85	0.132142	0.13	1780	1945



Figure 10. Zircon types from the Lajedo granodiorite. **a.** Small prismatic zircons, with rounded terminations and colorless. **b.** Small prismatic crystals with rounded terminations and with white aspect. **c.** Elongated and prismatic zircons with rounded termination.

Table 8. Sm-Nd whole rock analytical data of the Fé granitic gneiss and Lajedo granodiorite. See text for details.
 * = reference age.

Lab. number	Sample	Rock type	Sm (ppm)	Nd (ppm)	$^{147}\text{Sm}/^{144}\text{Nd}$	$^{143}\text{Sm}/^{144}\text{Nd}$	$f_{\text{Sm/Nd}}$	T_{DM} (Ma)	$\epsilon_{\text{Nd}(0)}$	$\epsilon_{\text{Nd}(t)}$	* $\epsilon_{\text{Nd}(2.12\text{ Ga})}$
2481	CAWT01-Fé	Granitic gneiss	7.28	39.84	0.1105 ± 4	0.511245 ± 13	-0.44	2.68	-27.2	-3.08	-3.9
3738	Lajedo	Granodiorite	1.18	6.279	0.1137 ± 4	0.511353 ± 13	-0.42	2.59	-25.0	-1.86*	-2.6

Table 9. Rb-Sr whole rock analytical data of the Fé granitic gneiss and Lajedo granodiorite. See text for details.
 * = reference age.

Rock	Rb (ppm)	Sr (ppm)	$^{87}\text{Sr}/^{86}\text{Sr}$	$^{87}\text{Sr}/^{86}\text{Sr}_{(\text{t})}$	$^{87}\text{Sr}/^{86}\text{Sr}_{(2.12\text{ Ga})}$
Fé granitic gneiss	305.2	99.3	0.957915	9.116	0.70497
Lajedo granodiorite	61.95	748.98	0.70841	0.228	0.70322

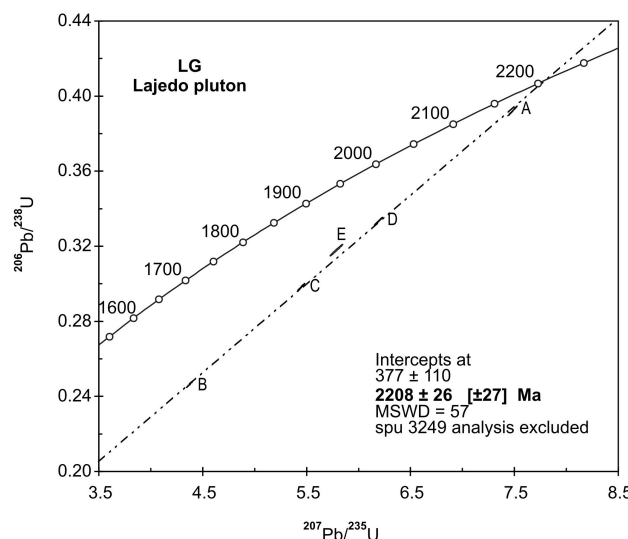


Figure 11. U-Pb diagram of LC-06 sample (Lajedo granodiorite). See text for details.

additional Nd/Sr data of roughly contemporary plutons (see Table 2) (Teixeira et al., 2005), as shown by the dashed circles. In this diagram all the isotopic data were recalculated according with the emplacement age of each pluton, except for the Cassiterita and Rio Grande plutons that yielded spurious $^{87}\text{Sr}/^{86}\text{Sr}_{(\text{t})}$ values (not shown).

The $f_{\text{Sm/Nd}}$ value of the Fé sample (CAWT-01) is -0.44, which agrees well with “usual” crustal parameters for Nd fractionation of granitic rocks. Its Sm-Nd T_{DM} single model age is 2.68 Ga and the $\epsilon_{\text{Nd}(2.19\text{ Ga})}$ value is -3.08. The Lajedo sample (Lajedo C-39) shows a comparable $f_{\text{Sm/Nd}}$ value (-0.42) and a significant younger T_{DM} single model age (2.59 Ga). Its

$\epsilon_{\text{Nd}(2.19\text{ Ga})}$ value is also significantly higher (-1.86), almost twice than that of the Fé pluton. The contrasting isotopic signatures may be dependent on varied mantle and crustal components acting in the magma genesis of each rock.

The Nd signature of the Fé granitic gneiss is consistent with some genetic influence from the hosted Paleoproterozoic Rio das Mortes greenstone belt, particularly from the metasedimentary rocks (see previous section), because the coeval mafic rocks yield significantly higher $\epsilon_{\text{Nd}(t)}$ values (between -1.5 and zero) than the analyzed granitic sample. We speculate that these sedimentary rocks might “preserve” an inherited Nd mean signature from the Archean/Paleoproterozoic passive continental margin, explaining thereby the T_{DM} age and strongly negative $\epsilon_{\text{Nd}(t)}$ value of the Fé intrusion. In contrast, the Nd evidence of the Lajedo granodiorite, hosted by the Nazareno greenstone belt, suggests a predominant role of a Paleoproterozoic juvenile end-member in its source, as similar as envisaged from the $\epsilon_{\text{Nd}(t)}$ value (-1.0) of one Nazareno andesite – see previous section. In addition we note that the $^{87}\text{Sr}/^{86}\text{Sr}_{(\text{t})}$ signatures of the investigated plutons are remarkable low: the Fé sample yields a $^{87}\text{Sr}/^{86}\text{Sr}_{(2.19\text{ Ga})}$ value of 0.70497 whereas the $^{87}\text{Sr}/^{86}\text{Sr}_{(2.20\text{ Ga})}$ ratio of the Lajedo sample is 0.70322. Both values, which are consistent with protholiths with low Rb/Sr ratios, suggest participation of either granulitic crust (short residence crustal materials) or mafic/ultramafic rocks in the magma source of these plutons. This inference agrees well again with the fact the Fé and Lajedo plutons contain amphibolite, pyroxenite xenoliths (see previous section).

Figure 12 shows the isotopic parameters of the investigated samples (Tables 8 and 9) together with data of roughly contemporary plutons of the Mineiro belt (see Table 2). All the samples fall in the depleted quadrant (III) of the correlation diagram, and do not tend toward EMII indicating

this component did not play an important role in the mantle composition at the Paleoproterozoic time. Such a depleted feature is basically due to the homogeneous, and remarkable low $^{87}\text{Sr}/^{86}\text{Sr}_{(t)}$ values (between 0.700 and 0.705) of the granitic samples, suggesting therefore a minimal action of upper continental components in the magma genesis.

The isotopic reservoirs of the Lajedo granodiorite ($\epsilon_{\text{Nd}(2.12 \text{ Ga})} = -2.6$; $^{87}\text{Sr}/^{86}\text{Sr}_{(2.12 \text{ Ga})} = 0.701$) and Fé granitic gneiss ($\epsilon_{\text{Nd}(2.12 \text{ Ga})} = -3.9$; $^{87}\text{Sr}/^{86}\text{Sr}_{(2.12 \text{ Ga})} = 0.700$) compare well with the data available for most of Mineiro belt plutons (see Table 2), as delineated by the dashed field A that exhibits characteristically low (-0.5 to -1.1) and intermediate (-2.3 to -3.3) negative $\epsilon_{\text{Nd}(t)}$ values. Therefore this group of samples probably originated by mixing of depleted mantle, as one end-member (rather than bulk earth), and a very subordinate low Rb/Sr, short-lived crustal component. Ávila et al. (2000) reported Nd/Sr analyses of coeval granitoid rocks displaying a significantly distinct, more negative $\epsilon_{\text{Nd}(t)}$ signature (from -5.4 to -11.8) – see field B (Figure 12). In consequence the isotopic reservoirs of the plutonic rocks of the Mineiro belt may be better explained by variable influence of DMM end-member combined with proportions of an enriched mantle-like component (e.g., EMI) in the magma genesis, with minor contribution from crustal components, such as the Rio das Mortes and Nazareno greenstone belt igneous rocks. The isotopic inferences are again consistent with the idea that the Paleoproterozoic plutonism of the Mineiro belt originated in an evolved island arc setting.

SUMMARY AND TECTONIC IMPLICATIONS

The Paleoproterozoic magmatic evolution of the Mineiro belt was dominated by voluminous calc-alkaline rocks, derived from mixing of predominant mantle (DMM and EMI) and crustal derived components (Ávila, 2000; Noce et al., 2000; Teixeira et al., 2005; Ávila et al., 2006).

The U-Pb age obtained for the Fé granitic gneiss (2191 ± 9 Ma) indicates that this is one of the oldest pre- to syntectonic intrusions recognized up to now in the north of the LSZ and Lenheiros fault, in conjunction with the nearby Gloria quartz-monadiorite (2188 ± 29 Ma; SHRIMP U/Pb age – Ávila et al., 2006) – see Figure 2. The emplacement of both plutons was succeeded by several other intrusions related similarly to such a tectonic phase, as supported by the available $^{207}\text{Pb}/^{206}\text{Pb}$ zircon evaporation ages: Cassiterita Trondjemite/Tonalite (2162 ± 10 Ma – Ávila et al., 2003), Rio Grande diorite (2155 ± 3 Ma; Cherman, 2002), Brumado diorite (2131 ± 4 Ma; Ávila, 2000) and Ritápolis granite (2121 ± 7 Ma; Ávila, 2000). Therefore this magmatic event has lasted ca. 70 Ma. In contrast, several pre- to syntectonic intrusions located southward of the Lenheiros – Rio das Mortes structure (Figure 2) show similar ages: Brito quartz-diorite: 2221 ± 2 Ma; São Sebastião da Vitória gabbro: 2220 ± 3 Ma; Brumado de Cima granodiorite: 2219 ± 2 Ma; Brumado de Baixo granodiorite: 2218 ± 3 Ma; Lajedo granodiorite: 2208 ± 26 Ma (Ávila et al., 2006; Teixeira and Ávila, 2007). From the above the different age patterns revealed within adjacent tectonic domains may represent plutonic polarity during the magmatic evolution of the Mineiro belt.

The Fé granitic gneiss and Lajedo granodiorite crosscut distinct greenstone belt units whereas their particular Nd characteristics compare well with the Nd signatures of coeval granitic intrusions occurring north and south from the Lenheiros structure (Teixeira et al., 2005; Teixeira and Ávila, 2007):

a. a group of plutonic rocks in south of the LSZ [Lajedo, Brumado de Cima and Brumado de Baixo and Brito (T_{DM} ages between 2.63-2.51 Ga)] exhibits less negative $\epsilon_{\text{Nd}(t)}$ values, ranging from -1.1 to -0.5, except for the Nazareno orthogneiss (-3.2);

b. the plutons located in north of the LSZ (Fé, Glória, Cassiterita, Rio Grande, Ritápolis and Brumado) exhibit more negative $\epsilon_{\text{Nd}(t)}$ values (-1.0; -2.3/-2.6; -3.3) and wider range of T_{DM} ages (2.41 to 2.68 Ga) than the former group.

In our view the contrasting isotopic features among these plutons are consistent with the hypothesis that a Paleoproterozoic intra-oceanic setting did exist southward of the Lenheiros structure which evolved to Andean-type arc environment along the passive continental margin of the São Francisco proto-Craton.

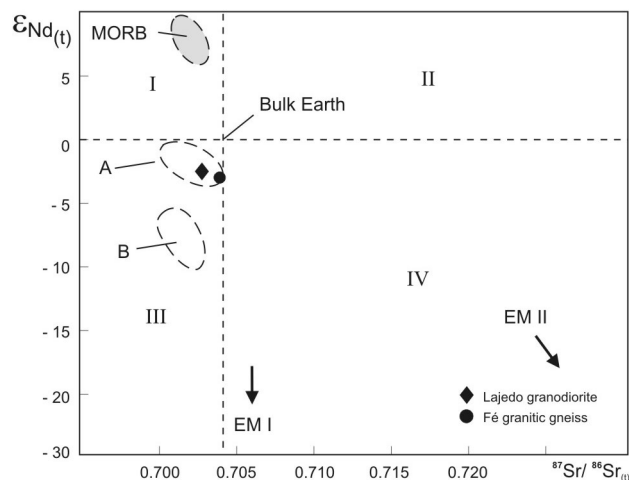


Figure 12. $\epsilon_{\text{Nd}(t)} \times {^{87}\text{Sr}}/{^{86}\text{Sr}}_{(t)}$ correlation diagram for the Lajedo and Fé samples. Isotopic fields of MORB and tectonically related plutons (dashed fields A and B) are also shown. The isotopic data (B field) not shown in Table 2 were recalculated from published references presented herein. See text for details.

The Nd isotopic characteristics of Fé and Lajedo plutons: negative $\epsilon_{\text{Nd(t)}}$ values (-3.1 and -1.9) and T_{DM} model ages (2.68 and 2.59 Ga, respectively) are coherent with such a model, in which mixing of Paleoproterozoic enriched-like (e.g., EMI) and DMM juvenile magmas coupled with some crustal component is commonly expected during generation of plutonic arc rocks. In addition the tectonic characteristics of the investigated rocks are comparable with that of the recognized pre- to syntectonic plutons in the studied area. As a whole the integrated radiometric data better constrain this phase in the Mineiro Belt in the investigated area, between 2.22 and 2.12 Ga.

Finally, the bulk of the Nd-Sr characteristics reported for several plutons in the Mineiro Belt (e.g., Noce et al., 2000; Avila et al., 2006; Teixeira and Ávila, 2007) suggest the crustal protholiths may be either Paleoproterozoic or Archean because the expected increasing interaction with the evolving Archean continental margin. Nevertheless, the proposed mantle-derived components (EMI, DMM) contributing to the granitoid sources reveal the important role of a Paleoproterozoic soft-collision/accretion event – herein envisaged for the Mineiro belt, southward from the LSZ. As a consequence of the belt evolution, regional metamorphism and deformation overprinted the Sul-Mineira province.

ACKNOWLEDGMENTS

This work was supported by Fundação de Amparo e Apoio à Pesquisa do Estado de São Paulo (FAPESP) under grants # 2004/1529-7 and 2004/11059-7. The authors thank the CPGeo technical staff for helping the analytical work. C. Ávila is grateful to Fundação Carlos Chagas Filho de Amparo à Pesquisa do Estado do Rio de Janeiro (FAPERJ; grant 170.023/2003). W. Teixeira and C. Ávila acknowledge the support of the Brazilian Research Council for Science and Technology (CNPq; grants 304300/03-9, 475673/04-2 and 308707/2006-0).

REFERENCES

- ALKMIM, F. F. O que faz um craton um craton? O Craton São Francisco e as revelações Almedianas ao delimitá-lo. In: MANTESSO-NETO, V.; BARTORELLI, A.; CARNEIRO, C. D. R.; BRITO-NEVES, B. B. *Geologia do continente sul-americano: evolução e obra de Fernando Flávio Marques de Almeida*. São Paulo: Beca, 2004. p. 17-35.
- ÁVILA, C. A. *Geologia, petrografia e geoquímica das rochas pré-cambrianas (Unidade Metadiorítica Ibitutinga e Unidade Metatrondjemítica Caburu) intrusivas nas rochas do Greenstone Belt Barbacena, São João Del Rei, Minas Gerais*. 1992. 265 f. Dissertação (Mestrado) - Departamento de Geologia, Universidade Federal do Rio de Janeiro, Rio de Janeiro, Rio de Janeiro, 1992.
- ÁVILA, C. A. *Geologia, petrografia e geocronologia de corpos plutônicos paleoproterozóicos da borda meridional do Craton São Francisco, região de São João del Rei, Minas Gerais*. 2000. 401 f. Tese (Doutorado) – Departamento de Geologia, Universidade Federal do Rio de Janeiro, Rio de Janeiro, 2000.
- ÁVILA, C. A.; TEIXEIRA, W.; PEREIRA, R. M. Geologia e petrografia do quartzo monzodiorito Glória, cinturão mineiro, porção sul do Craton do São Francisco, estado de Minas Gerais. *Arquivos do Museu Nacional*, Rio de Janeiro, v. 62, p. 83-98, 2004.
- ÁVILA, C. A.; VALENÇA, J. G.; MOURA, C. A. V.; TEIXEIRA, W. Geoquímica e geocronologia do Diorito Brumado, região de São João del Rei, Minas Gerais. In: CONGRESSO BRASILEIRO GEOQUÍMICA, 7., 1999, Porto Seguro. *Boletim Resumos Expandidos...* Porto Seguro: SBGq, 1999. v. 1, p. 300-302.
- ÁVILA, C. A.; VALENÇA, J. G.; MOURA, C. A. V.; KLEIN, V. C.; PEREIRA, R. M. Geoquímica e idade do trondjemito cassiterita, borda meridional do Craton São Francisco, Minas Gerais. *Arquivos do Museu Nacional*, Rio de Janeiro, v. 61, p. 267-284, 2003.
- ÁVILA, C. A.; TEIXEIRA, W.; CORDANI, U. G.; BARRUETO, H. R.; PEREIRA, R. M.; MARTINS, V. T. S.; DUNYI, L. The gloria quartz-monzodiorite: isotopic and chemical evidence of arc-related magmatism in the central part of the paleoproterozoic mineiro belt, Minas Gerais state, Brazil. *Anais da Academia Brasileira de Ciências*, Rio de Janeiro, v. 78, p. 543-556, 2006.
- ÁVILA, C. A.; VALENÇA, J. G.; TEIXEIRA, W.; BARRUETO, H. R.; CORDANI, H. G.; MOURA, C. A. V.; PEREIRA, R. M.; MARTINS, V. T. S. Geocronologia U/Pb e Pb/Pb da Suíte Serrinha: implicações para a evolução paleoproterozóica da margem sul do Craton São Francisco. In: SIMPÓSIO DE VULCANISMO E AMBIENTES ASSOCIADOS, 3., 2005, Cabo Frio. *Anais...* Cabo Frio: SBG, 2005. v. 1, p. 357-361.
- BASEI, M. A. S.; SIGAJUNIOR, O.; SATO, K.; SPROESSER, W. M. A instalação da metodologia U-Pb na Universidade de São Paulo. Princípios metodológicos, aplicações e resultados obtidos. *Anais da Academia Brasileira de Ciência*, Rio de Janeiro, v. 67, p. 221-237, 1995.
- BOYNTON, W. V. Cosmochemistry of the rare earth element:

meteorite studies. In: HENDERSON, P. *Rare earth element geochemistry*. Amsterdam: Elsevier, 1984. p. 63-114.

BROWN, G C.; THORPE, R. S.; WEBB, P. C. The geochemical characteristics of granitoids in contrasting arcs and comments on magma sources. *Journal of Geological Society of London*, London, v. 141, p. 411-426, 1984.

CAMPOS, J. C. S.; CARNEIRO, M. A.; BASEI, M. A. S. U-Pb evidence for late Neoarchean crustal reworking in the southern São Francisco craton (Minas Gerais, Brazil). *Anais da Academia Brasileira Ciências*, Rio de Janeiro, v. 75, p. 497-511, 2003.

CARNEIRO, M. A. *O complexo metamórfico Bonfim Setentrional (Quadrilátero Ferrífero, Minas Gerais): litoestratigrafia e evolução geológica de um segmento de crosta continental do Arqueano*. 1992. 233 f. Tese (Doutorado) - Instituto de Geociências, Universidade de São Paulo, São Paulo, 1992.

CHERMAN, A. F. *Geologia e petrografia de áreas dos Greenstone Belt Rio Capivari-Rio das Mortes e Itumirim-Tiradentes e rochas granítoides associadas, entre Nazareno e Lavras (estado de Minas Gerais)*. 2002. 161 f. Dissertação (Mestrado) - Departamento de Geologia, Universidade Federal do Rio de Janeiro, Rio de Janeiro, 2002.

CHERMAN, A. F. *Geologia, petrografia e geocronologia de ortognaisse paleoproterozóicos da borda meridional do Craton do São Francisco, na região entre Itumirim e Nazareno, M.G.* 2004. 259 f. Tese (Doutorado) - Departamento de Geologia, Universidade Federal do Rio de Janeiro, Rio de Janeiro, 2004.

CHERMAN, A. F.; VALENÇA, J. G. Geologia e geocronologia dos ortognaisse paleoproterozóicos da borda meridional do Craton do São Francisco, entre as cidades de Nazareno e Lavras, sul de Minas Gerais. In: SIMPÓSIO SOBRE CRATON SÃO FRANCISCO, 3., 2005, Salvador. *Anais...* Salvador: SBG, 2005. v. 1, p. 147-150.

De PAOLO, D. J. Nd isotopic studies; some new perspectives on earth structure and evolution. *Transactions of American Geophysics Union*, v. 62, p. 137-140, 1981.

De PAOLO, D. J.; LINN, A. M.; SCHUBERT, G. The continental crustal age distribution; methods of determining mantle separation ages from Sm-Nd isotopic data and application to the Southwestern United States. *Journal of Geophysical Research*. Washington, v. B 96, p. 2071-2088, 1991.

HARTMANN, L. A.; ENDO, I.; SUITA, M. T.; SANTOS, J.

O. S.; FRANTZ, J. C.; CARNEIRO, M. A.; MCNAUGHTON, N. J.; BARLEY, M. E. Provenance and age delimitation of quadrilátero ferrífero sandstones based on zircon U-Pb isotopes. *Journal of South American Earth Science*, Oxford, v. 20, p. 273-285, 2006.

IRVINE, T. N.; BARAGAR, W. R. A. A guide to the chemical classification of common volcanic rocks. *Canadian Journal of Earth Sciences*, Ottawa, v. 8, p. 523-548, 1971.

LeMAITRE, R. W. *A classification of igneous rocks and glossary of terms*. (Recommendations of the international union of geological sciences subcommission on the systematics of igneous rocks). Oxford: Blackwell, 1989. 193 p.

LUDWIG, K. G. Isoplot 3.0: a geochronological toolkit for microsoft excel. *Berkeley Geochronology Center Special Publication*. v. 4, p. 71, 2000.

MACHADO, N.; CARNEIRO, M. A. U-Pb evidence of late archean tectono-thermal activity in the southern São Francisco shield, Brazil. *Canadian Journal of Earth Sciences*, Ottawa, v. 29, p. 2341-2346, 1992.

MACHADO, N.; SCHRANK, A.; NOCE, C. M.; GAUTHIER, G. Ages of detrital zircon from archean-paleoproterozoic sequences: implications for Greenstone Belt setting and evolution of a transamazonian foreland basin in quadrilátero ferrífero, southeast Brazil. *Earth Planetary Science Letters*, Amsterdam, v. 141, p. 259-276, 1996.

MANIAR, P. D.; PICOLLI, P. M. Tectonic discrimination of granitoids. *Geological Society of American Bulletin*, Boulder, v. 101, p. 635-643, 1989.

MARTIN, H. Petrogenesis of archean trondhjemites, tonalites and granodiorites from eastern Finland: major and trace element geochemistry. *Journal of Petrology*, v. 28, n. 5, p. 921-953, 1987.

NOCE, C. M. *Geocronologia dos eventos magmáticos, sedimentares e metamórficos na região do quadrilátero ferrífero, Minas Gerais*. 1995. 128 f. Tese (Doutorado) - Instituto de Geociências, Universidade de São Paulo, São Paulo, 1995.

NOCE, C. M.; MACHADO, N.; TEIXEIRA, W. U/Pb Geochronology of gnaisses and granitoids in the quadrilátero ferrífero (southern São Francisco Craton): age constraints for archean and paleoproterozoic magmatism and metamorphism. *Revista Brasileira de Geociências*, São Paulo, v. 28, p. 95-102, 1998.

NOCE, C. M.; TEIXEIRA, W.; QUÉMÉNEUR, J. J. G.; MARTINS, V. T. S.; BOLZACHINI, E. Isotopic signatures of paleoproterozoic granitoids from the southern São Francisco Craton and implications for the evolution of the transamazonian orogeny. *Journal of South American Earth Sciences*, Oxford, v. 13, p. 225-239, 2000.

NOCE, C. M.; ZUCCHETI, M.; BALTAZAR, O. F.; ARMSTRONG, R.; DANTAS, E.; RENGER, F. E.; LOBATO, L. M. Age of felsic volcanism and the role of ancient continental crust in the evolution of the neoarchean Rio das Velhas Greenstone belt (quadriátero ferrífero, Brazil): U-Pb zircon dating of volcaniclast graywackes. *Precambrian Research*, Amsterdam, v. 141, p. 67-82, 2005.

O'CONNOR, J. T. A classification of quartz-rich igneous rocks based on feldspar ratios. *United States Geological Survey Professional Paper*, Denver, v. 525-B, p. 79-84, 1965.

PECCERILLO, R.; TAYLOR, S. R. Geochemistry of eocene calc-alkaline volcanic rocks from Kastamonu area, northern Turkey. *Contributions to Mineralogy and Petrology*, Berlin, v. 58, p. 63-81, 1976.

PEARCE, J. A.; HARRIS, N. B. W.; TINDLE, A. G. Trace element discrimination diagrams for the tectonic interpretation of granitic rocks. *Journal of Petrology*, Oxford, v. 25, p. 956-983, 1984.

PIRES, F. R. M.; RIBEIRO, A.; BARBOSA, M. I. M. Distribuição do “Greenstone Belt” Barbacena na região de São João Del Rei, Minas Gerais. In: CONGRESSO BRASILEIRO GEOLOGIA, 36., 1990, Natal. *Anais...* Natal: SBG, 1990. v. 5, p. 2941-2951.

QUÉMÉNEUR, J. J. G.; BARAUD, E. R. Geologia da área pegmatítica de São João Del Rey, Minas Gerais, Brasil. In: CONGRESSO LATINO AMERICANO DE GEOLOGIA, 5., 1982, Buenos Aires. *Actas...* Buenos Aires, 1982. v. 1, p. 39-53.

QUÉMÉNEUR, J. J. G.; NOCE, C. M. Geochemistry and petrology of felsic and mafic suite related of the paleoproterozoic transamazonian orogeny in Minas Gerais, Brazil. *Revista Brasileira de Geociências*, São Paulo, v. 30, n. 1, p. 87-90, 2000.

RIBEIRO, A.; TROUW, R. A. J.; ANDREIS, R. R.; PACIULLO, F. V. P.; VALENÇA, J. G. Evolução das bacias proterozóicas e o termo-tectonismo brasiliano na margem sul do Craton do São Francisco. *Revista Brasileira de Geociências*, São Paulo, v. 25, n. 4, p. 235-248, 1995.

SATO, K; TASSINARI, C. C. G.; KAWASHITA, K.; PETRONILHO, L. O método geocronológico Sm-Nd no IG/USP e suas aplicações. *Anais da Academia Brasileira de Ciências*, Rio de Janeiro, v. 67, n. 3, p. 313-336, 1995.

SILVA, M.A. *Geologia e petrografia do corpo metagábrico pré-cambriano de São Sebastião da Vitória, Minas Gerais*. 1996. 125 f. Dissertação (Mestrado) – Departamento de Geologia, Universidade Federal do Rio de Janeiro, Rio de Janeiro, 1996.

SÖLLNER, F.; TROUW, R. A. J. The Andrelândia depositional cycle (Minas Gerais/Brazil), a post-transamazonic sequence south of the São Francisco Craton: evidence from U-Pb dating on zircons of a metasediment. *Journal of South American Earth Sciences*, Oxford, v. 10, n. 1, p. 21-28, 1997.

STRECKEISEN, A. To each plutonic rock, its proper name. *Earth Science Review*, Amsterdam, v. 12, p. 1-33, 1976.

TAYLOR, S. R.; McLENNAN, S. M. *The continental crust: its composition and evolution*. Oxford: Blackwell, 1985. 234 p.

TEIXEIRA, W.; CORDANI, U. G.; NUTMAN, A. P.; SATO, K. Polyphase archean evolution in the Campo Belo Metamorphic Complex, southern São Francisco Craton, Brazil: shrimp and U-Pb zircon evidence. *Journal of South American Earth Science*, Oxford, v. 11, n. 3, p. 279-289, 1998.

TEIXEIRA W.; SABATÉ, P.; BARBOSA, J.; NOCE, C. M.; CARNEIRO, M. A. Archean and paleoproterozoic evolution of the São Francisco Craton, Brazil. In: CORDANI, U. G.; MILANI, E. J.; THOMAZ FILHO, A.; CAMPOS, D. A. *Tectonic evolution of South America*. Rio de Janeiro: SBG, 2000. p. 101-137. (Special Publication).

TEIXEIRA W.; ÁVILA, C. A.; CORDANI, U. G.; MARTINS, V. T. S.; VALENÇA, J. G. Dados isotópicos (U/Pb, Pb/Pb, Sm/Nd, Rb/Sr) do plutônio paleoproterozóico do Cinturão Mineiro, porção meridional do Craton São Francisco: implicações tectônicas. In: SIMPÓSIO SOBRE O CRATON SÃO FRANCISCO, 3., 2005, Salvador. *Anais...* Salvador: SBG, 2005. v. 1, p. 174-177.

TEIXEIRA, W.; ÁVILA, C. A. Evolução geodinâmica do Cinturão Mineiro: revisão do conhecimento após duas décadas de estudos. In: SIMPÓSIO DE GEOLOGIA DO SUDOESTE, 10., 2007, Diamantina. *Programação e Livro de Resumos*, SBG: MG/RJ/SP, 2007. p. 84.

TOLEDO, C. L. B. *Evolução geológica das rochas maficas e ultramáficas no Greenstone Belt Barbacena, na região*

de Nazareno, MG. 2002. 307 f. Tese (Doutorado) – Instituto de Geociências, Universidade Estadual de Campinas, Campinas, 2002.

TROUW, R. A. J.; PANKHUST, R. J. Idades radiométricas ao sul do Craton do São Francisco: região da folha Barbacena, Minas Gerais. In: SIMPÓSIO SOBRE O CRATON DO SÃO FRANCISCO, 2., 1993, Salvador. *Anais...* Salvador: SBG 1993. v. 1, p. 260-262.

TROUW, R. A. J.; RIBEIRO, A.; PACIULLO, F. V. P. Contribuição à geologia da Folha Barbacena - 1: 250.000. In: CONGRESSO BRASILEIRO GEOLOGIA, 34., 1986, Goiânia. *Anais...* Goiânia: SBG 1986. v. 2, p. 974-986.